https://doi.org/10.1016/j.carbon.2018.11.074

Ultrafast Response of Spray-on Nanocomposite Piezoresistive Sensors to Broadband Ultrasound

Yaozhong Liao[a, 1], Feng Duan[a, b, c, 1], Hongti Zhang[d], Yang Lu[d,e], Zhihui Zeng[f], Menglong Liu[g], Hao Xu[h], Chang Gao[h], Li-min Zhou[a], Hao Jin[b], Zhong Zhang[b, **] and Zhongqing Su[a, *]

[a] Department of Mechanical Engineering, The Hong Kong Polytechnic University, Kowloon, Hong Kong SAR

[b] CAS Key Laboratory of Nanosystem and Hierarchical Fabrication, National Center for Nanoscience and Technology, Beijing 100190, P. R. China

[c] University of Chinese Academy of Sciences, Beijing 100049, P. R. China

[d] Department of Mechanical and Biomedical Engineering, City University of Hong Kong, 83 Tat Chee Avenue, Kowloon, Hong Kong SAR

[e] Centre for Advanced Structural Materials, City University of Hong Kong, 83 Tat Chee Avenue, Kowloon, Hong Kong SAR

[f] School of Materials Science and Engineering, Nanyang Technological University, 50 Nanyang Avenue, Singapore 639798, Singapore

[g] Institute of High Performance Computing, A*STAR, Singapore 138632, Singapore

[h] School of Aeronautics and Astronautics, Dalian University of Technology, Dalian, 116024, P. R. China

(initially submitted on 2nd August 2018; revised and re-submitted on 20th October 2018; further revised and re-submitted on 21st November 2018)

* Corresponding author.
** Corresponding author.
E-mail address: zhongqing.su@polyu.edu.hk **(Z. Su),** zhong.zhang@nanoctr.cn **(Z. Zhang).**
[1] These authors contributed equally to this work.

Abstract: We present a nano-engineered thin-film-type piezoresistive sensor, coatable or sprayable on a medium surface for *in-situ* acquisition of broadband ultrasound up to 1.4 MHz – a trait of nanocomposite-based piezoresistive sensing devices that has until now not been discovered and explored. With polyvinylidene fluoride as the matrix, fabrication of the spray-on sensor is attempted in a comparative manner, with multiscale nanofillers ranging from zero-dimensional carbon black, through one-dimensional multiwalled carbon nanotubes, to two-dimensional graphene nanoparticles. With a morphologically optimal nano-architecture, the quantum tunneling effect can be triggered in the percolating nanofiller network when ultrasound signals traverse the sensor, inducing dynamic alteration in the piezoresistivity manifested by the sensor. *In-situ* morphological analysis and experiment reveal high fidelity, ultrafast responses, and high sensitivity of the sensor to dynamic disturbance, from static strain to ultrasound in a regime of megahertz yet with an ultralow magnitude (of the order of microstrain or nanostrain). These findings are remarkable as no other investigation has probed the response of nanocomposite piezoresistive sensors over such a broad frequency spectrum.

Keywords: spray-on sensor; nanocomposite piezoresistive sensor; broadband ultrasound; ultrafast response

1. Introduction

Sensing – the infrastructure of a cognitive system either biological or artificial – plays the most rudimentary yet pivotal role in feeling changes of self-condition or fluctuation of ambient factors [1-10], on which basis apperception and cognition are developed. The recent quantum leap in nanotechnology has blazed a trail in contriving, designing, and optimizing nanocomposite-inspired sensing devices. Deployable in diverse modalities such as film, fiber, and porous entities, nanocomposite sensors are lightweight, resilient, sensitive, stretchable, and easily fabricated,

offering appealing perspectives to entertain demanding measurement needs [11-16]. Prevailing nanocomposite sensors are demonstrably responsive to deformation of the order of millistrain engendered by a static load or a dynamic disturbance with a frequency up to several hundred hertz, in that a strain of that class suffices to alter nanofiller-formed conductive networks in sensors, resulting in measurable change [17-20].

Nevertheless, this sensor genre, as typified by nanocomposite piezoresistive sensors, is in general unable to respond to a dynamic disturbance beyond several kilohertz (kHz), let alone megahertz (MHz) ultrasound. One of the key barriers here is that the ultraweak energy carried by a high-frequency dynamic disturbance (e.g., an ultrasound signal) can lead to deformation in the order of microstrain or even nanostrain, which, under most circumstances, is inadequate to provoke a phenomenal change in piezoresistivity that can be measured by a piezoresistive sensor. This challenge has engendered intensive endeavors to enhance the responsive capability of nanocomposite piezoresistive sensors to dynamic disturbance with frequencies beyond kHz. Hitherto, the fastest response of a nanocomposite-based piezoresistive sensor has reportedly reached 2 kHz [21] ~ 10 kHz [22].

Facilitated by recent breakthroughs in nanomaterials, electronic packaging, and measurement technology, we have developed a rapid-responsive, thin-film-type nanocomposite piezoresistive sensor by exploiting the tunneling effect in the percolating nanofiller network that is triggered by a traversing ultrasound, whereby high-frequency ultrasound signals can be acquired [23-27]. This new breed of sensor has been demonstrated responsive to a dynamic disturbance up to 1.4 MHz – much higher than other available nanocomposite sensors. The perceived ultrasound signals are accurate and faithful, without discernible hysteresis or deviation in waveform. To put it into perspective, **Fig. 1** chronologically compares the currently prevailing nanocomposite piezoresistive sensors against our sensor, in terms of their respective responsive frequency maxima [1, 11, 21, 22, 28-32].

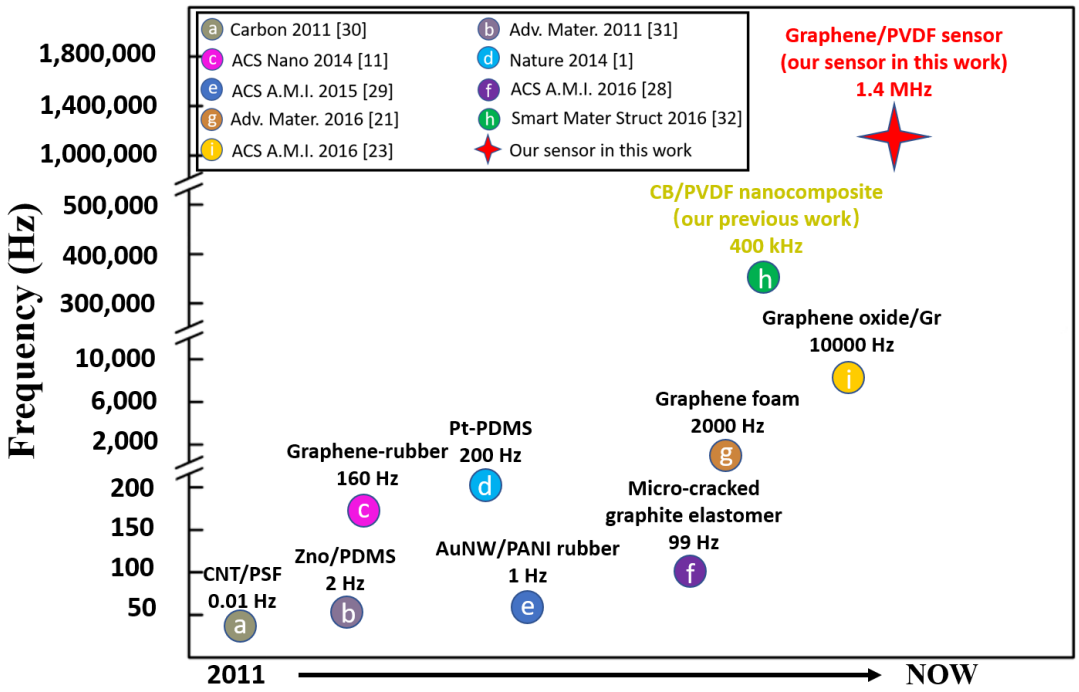

Fig. 1. Chronological comparison of nanocomposite piezoresistive sensors developed since 2011 (including that reported in this Carbon), in terms of their respective responsive frequency maxima [1, 11, 21, 22, 28-32].

By extending our earlier effort in exploring high-frequency-responsive nanocomposite sensors [32], in this study we attempt nanocomposite sensors in a comparative manner, with multiscale nanofillers ranging from one-dimensional (1-D) multiwalled carbon nanotubes (MWCNTs) with a low specific surface area (SSA) of the order of hundreds of square meters per gram (m^2/g), through zero-dimensional (0-D) carbon black (CB) with a medium SSA less than 900 m^2/g, to two-dimensional (2-D) graphene with a high SSA from 1000 to 3000 m^2/g, to advance insight into the sensing capability and sensing mechanism of nanocomposite piezoresistive sensors when they respond to high-frequency dynamic disturbance and ultrasound in particular [33].

The findings obtained are remarkable and promising, showing that the fabricated sensors, with properly selected nanofillers and a morphologically optimized nanostructure, can respond to broadband excitations, from static strain to ultrasound up to 1.4 MHz, yet with ultralow magnitude – a trait of nanocomposite-based piezoresistive sensing devices that has not until now been fully

explored. Taking a step further and making use of the alluring features of the developed nanocomposites including extra-lightweight and rapid prototyping, the sensors are deposited directly onto a medium surface, in conjunction with screen-printed electronic circuits, to form a dense sensing network for *in-situ* acquisition of broadband ultrasound. This study spotlights new application prospects of nanocomposite-inspired sensors in burgeoning ultrasonics-based health monitoring (for both human and engineering assets), tactile sensing, and wearable apparatus, in lieu of conventional sensors [32, 34-35].

2. Results and Discussion

2.1. *Preparation of nanocomposite ink*

Nanofillers with various degrees of specific surface were prepared, including (i) MWCNTs (FloTube™ 7000, average tube diameter ~6–10 nm, length ~50 µm, SSA ~250 m^2/g, purity > 95 wt.%, supplied by Cnano Technology Ltd.), (ii) CB (N220, average particle diameter ~80 nm, SSA ~600 m^2/g, supplied by CABOT Co.), and (iii) graphene (thickness ~1 nm, diameter 50 µm, SSA ~1200 m^2/g, purity > 99 wt.%, supplied by TANFENG Ltd.). A standard solution-mixing process was used to compound nanofillers with polyvinylidene fluoride (PVDF; Kynar k721, density 1.74 g/cm3, melting point ~158 ºC, ARKEMA), dissolved in 1-Methyl-2-pyrrolidinone (NMP) with a weight ratio of 20:80, in a mechanical stirrer at 800 rpm for 120 min. For each type of nanofiller, nanocomposites with a range of mass ratios of nanofiller to matrix were fabricated. An ultrasonic cell disrupter was used to agitate nanofillers in the PVDF by 'peeling off' individual nanofillers located at the outer part of the nanofiller bundles or in agglomerates, leading to even and uniform dispersion of nanofillers in matrix. After a standard degassing process to remove trapped air bubbles (at 60 ºC for 30 min), nanocomposite ink was prepared and could be deposited onto engineering structures directly or onto polymer substrates as a film ~5 µm in thickness using spray-coating technology.

2.2. *Morphological characteristics of fabricated nanocomposite sensors*

In quest of the sensitivity of percolating networks formed by nanofillers of various modalities to a broadband dynamic disturbance, nanoparticles with different degrees of SSA, varying from ~100 m^2/g (MWCNTs) to >1000 m^2/g (graphene), were compounded with PVDF as matrix, to prepare nanocomposites in a comparative manner. Emphasis was laid on dispersion of nanofillers in the matrix to create an even and stable conductive percolating network in the nanocomposites. **Fig. 2** shows scanning electron microscope (SEM) images of three representative genres of the nanocomposites at their respective percolation thresholds that were predetermined by calibrating the electrical conductivity of the nanocomposites against the wt.% of the nanofiller, as shown in **Fig. 2**a. As seen in **Fig. 2**a, the percolation thresholds are ~1 wt.% for MWCNTs-based, ~6.5 wt.% for CB-based, and ~1 wt.% for graphene-based nanocomposites. Massive entanglements or aggregations of nanofillers in the matrix can be observed for the nanocomposites with MWCNTs (**Fig. 2**b) or CB (**Fig. 2**c) as nanofillers, compared with the even dispersion when graphene nanoparticles are used as nanofillers (**Fig. 2**d). It is also noteworthy that all the experimental conditions during conductivity measurement were kept consistent for all nanocomposite types, including the electrode use and applied voltage.

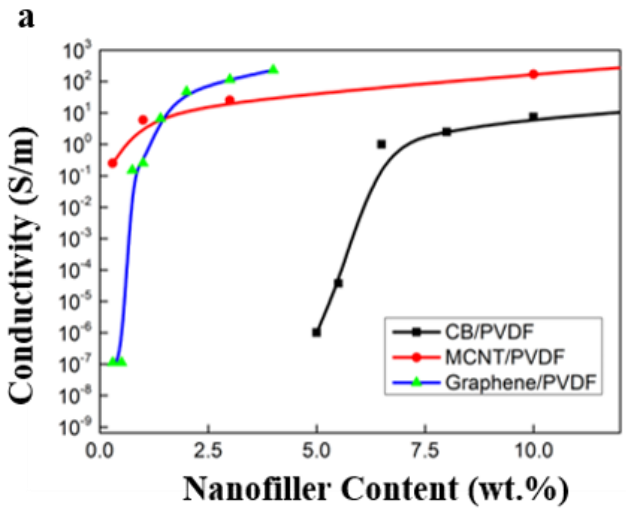

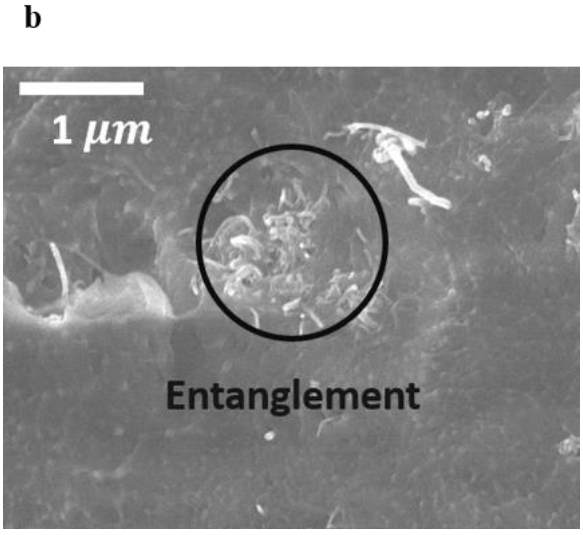

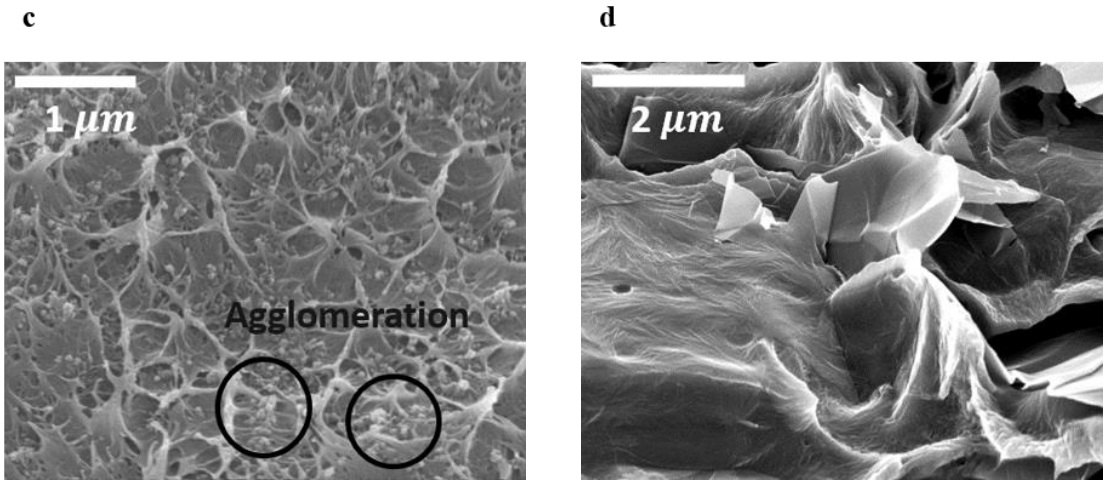

Fig. 2. (a) Correlation between the measured electrical conductivity of three genres of nanocomposites and wt.% of nanofiller; and SEM images (obtained using a field emission SEM (JSM-7500F, JEOL Ltd.)) of produced nanocomposites at their respective percolation thresholds with low, medium, and high degrees of SSA, (b) ~250 m^2/g (MWCNTs, 1wt.%), (c) ~600 m^2/g (CB, 6.5 wt.%), and (d) ~1200 m^2/g (graphene, 1 wt.%).

Notably, when compared with the measurement of static strain or low-frequency dynamic strain, the acquisition of ultrasound using nanocomposite piezoresistive sensors faces a twofold challenge: i) responsive sensitivity to an ultralow magnitude (of the order of microstrain or even nanostrain) and ii) responsive frequency beyond several hundred kHz.

2.3. *Sensitivity to ultralow magnitude*

Using a dynamic mechanical testing platform (TA Q800, TA Instruments), a series of axial compression tests was conducted on the three representative nanocomposite genres with MWCNTs, CB, and graphene as nanofiller. In the tests, each sample was trimmed to 5.11 mm in length, 5.11 mm in width and 1.8 mm in thickness. A nanoscale strain was generated and applied on each sample. The displacement of the compression head (moving at a speed of 1 μm/s) and the

accordingly engendered compressive force applied on the sample were prudently determined so that both could reach their respective extrema simultaneously. Notably, the displacement and consequently induced force respectively resembled the deformation and load induced to the sample by a typical ultrasound signal. We take the sample with graphene as nanofiller as an example, in which the maximum displacement and accordingly induced current measured *in situ* are ~5000 nm and ~ 4.744 μA, respectively. A linear correlation between the applied force and the *in-situ* measured current can be observed for all nanocomposite types; **Fig. 3** shows that of the graphene/PVDF-based nanocomposites. This observation demonstrates that the nanocomposites, properly prepared, are sufficiently and precisely sensitive to a dynamic disturbance down to the order of nanoscale strains. On the basis of our earlier simulation results [36] and quarter Wheatstone bridge configuration, the strain induced by a typical ultrasound signal varies from hundreds of nanostrains to several microstrains.

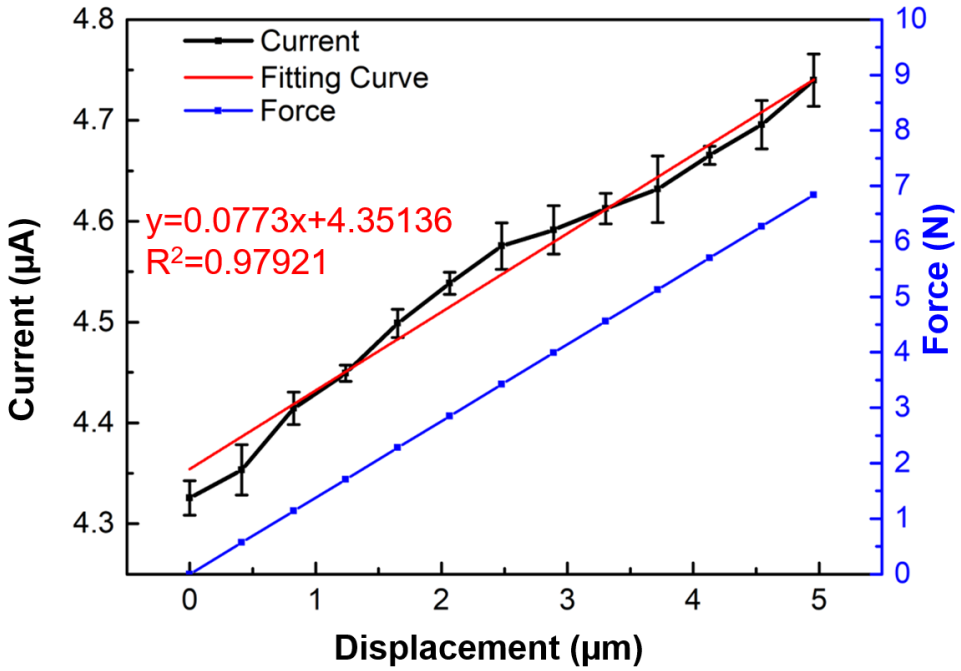

Fig. 3. *In-situ* nanostrain compression test results: correlation between applied force and *in-situ* measured current in graphene/PVDF-based nanocomposites

2.4. *Response to high frequency (up to 2 kHz)*

Nevertheless, the frequency of the dynamic load applied on the nanocomposite samples in the above nano-compression tests was obviously far below an ultrasonic frequency. To extend the investigation to a higher frequency domain, dynamic electromechanical excitation-response tests were implemented from static to dynamic up to 2 kHz.

The test for measuring quasi-static dynamic response was performed using a semiconductor characterization system (4200-SCS, Keithley Instruments, Inc.) on a dynamic mechanical testing platform (TA Q800, TA Instruments). A cyclic load windowed in a ramp strain mode (1.0%/min) was applied on the nanocomposite samples, to generate a strain up to 1%. Representatively and comparatively, **Fig. 4**a shows the measured change in resistance of the three nanocomposite genres (MWCNT, CB, and graphene), when undergoing a low-frequency cyclic load at 8 microhertz (mHz). It can be observed that the MWCNT-based nanocomposites fail to conform to the load, showing a deviated and distorted waveform; this contrasts with the other two nanofiller types that exhibit faithful adherence to the load without observable hysteresis or wave distortion. The thermal stability of the graphene/PVDF-based nanocomposites was further examined. In the range from -90 ℃ to 75 ℃, **Fig. 4**b shows the change in response energy of the nanocomposites when a strain of 0.5% is applied on the graphene/PVDF-based nanocomposite sample, accentuating the slight dependence of the material on temperature within a range between -40 ℃ and 75 ℃, owing to the stable nanostructure of the matrix (PVDF) in this range; however, a dramatic increase occurs in the resistance change ratio of the material in a cryogenic environment (below -40℃), that can be attributed to the contraction of the matrix under low temperature that consequently results in cracking and reduced friction between graphene flakes and PVDF.

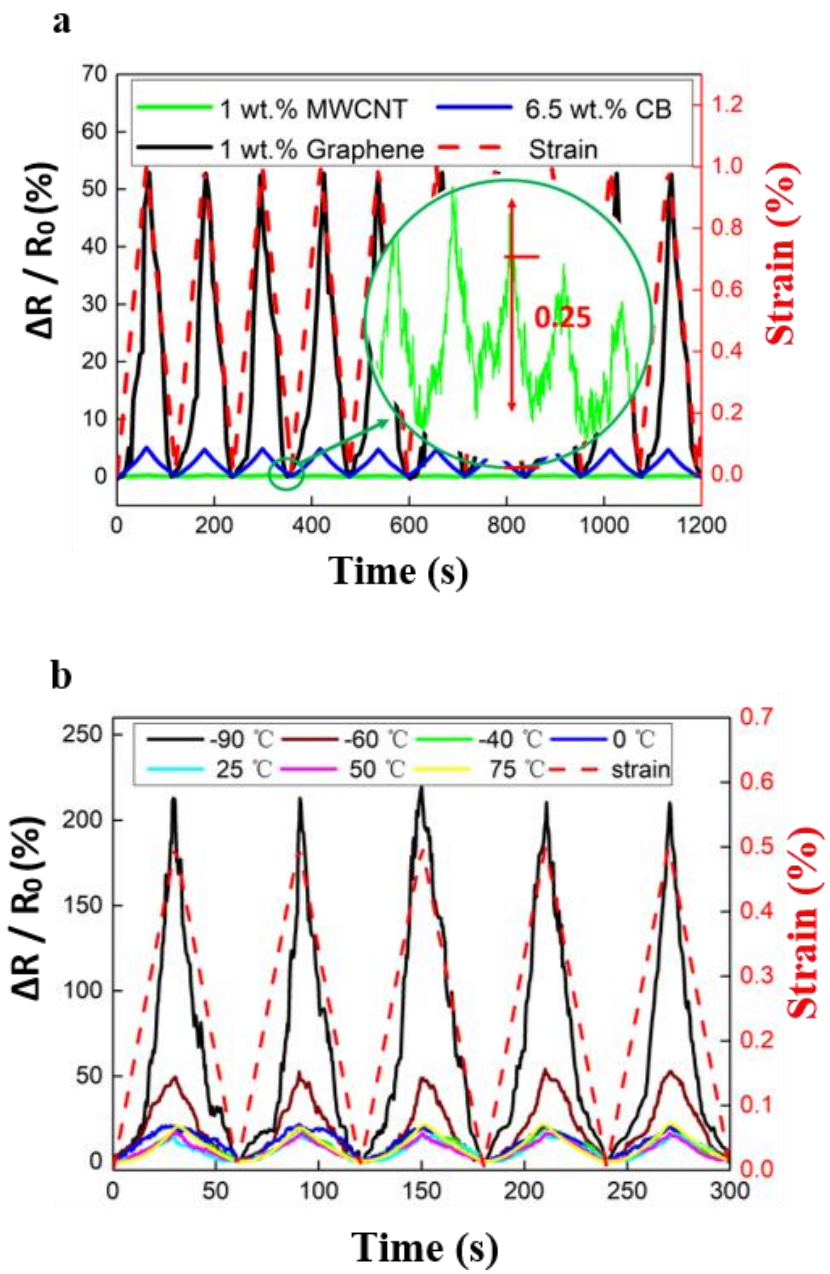

Fig. 4. Electromechanical test results: (a) responses of nanocomposite samples of three nanofiller genres to a quasi-static dynamic load at 8 mHz; (b) response of graphene/PVDF-based nanocomposite sample to a quasi-static dynamic load at 16 mHz under different temperatures, with reference to measurement from strain gauge.

A testing system, pictured in Fig. **5**a, was configured for acquiring the responses of samples under excitations in the range 100–2000 Hz, consisting mainly of a signal amplification module integrating a Wheatstone bridge with adjustable resistors compatible with the electrical resistance of

the developed sensor, an electronic amplifier circuit, a series of filters and a signal conversion circuit for converting measured piezoresistivity to electrical signals, a waveform generator (HIOKI® 7075) (for generating a continuous sinusoidal signal), a power amplifier (B&K® 2706), an electromechanical shaker (B&K® 4809) (for introducing vibration to a structure), and an oscilloscope (Agilent® DSO9064A). The three genres of fabricated sensors (length 10 mm, width 5 mm, thickness ~5 μm) were deposited onto a clamped cantilevered beam made of glass-fiber/epoxy composites (length 290 mm, width 40 mm, thickness 2 mm) along with a strain gauge (gauge factor: 2.07) adhered to the beam for comparison, see **Fig 5**a. The shaker excited the beam through a bonded point, with a sinusoidal signal sweeping from 100 to 2000 Hz.

With a load of a higher frequency (200 Hz), the sample with graphene as the nanofiller outperformed its counterparts using other types of nanofillers, clinging to the load and conveying the strongest responsive energy, as shown in **Fig. 5**b. With the highest sensitivity to external loads, the graphene/PVDF-based nanocomposites were chosen for further investigation. With a further increase in the excitation frequency to 2 kHz, the graphene/PVDF-based nanocomposite samples retained their faithful responses to the excitation, as shown in **Fig. 5**c. Together, these observations highlight the dynamic stability, measurement repeatability, and response reversibility of graphene/PVDF-based nanocomposites at ~1 wt.% in responding to high-frequency (up to 2 kHz) dynamic strains, without detectable waveform distortion and response hysteresis. No obvious discrepancy can be observed among the signals acquired by those sensors compared with the strain gauge in **Fig. 5**b. No obvious discrepancy can be observed between the signals acquired by the nanocomposite sensors with different nanofillers and the strain gauge, as shown in **Fig. 5**b. Note that a precise half-cycle of phase difference between the signals acquired by the graphene/PVDF-based nanocomposite sensor and those measured by the strain gauge can be observed, which is attributed to the fact that the sensor and the strain gauge are symmetrically positioned on two sides of the beam, as pictured in **Fig 5**a.

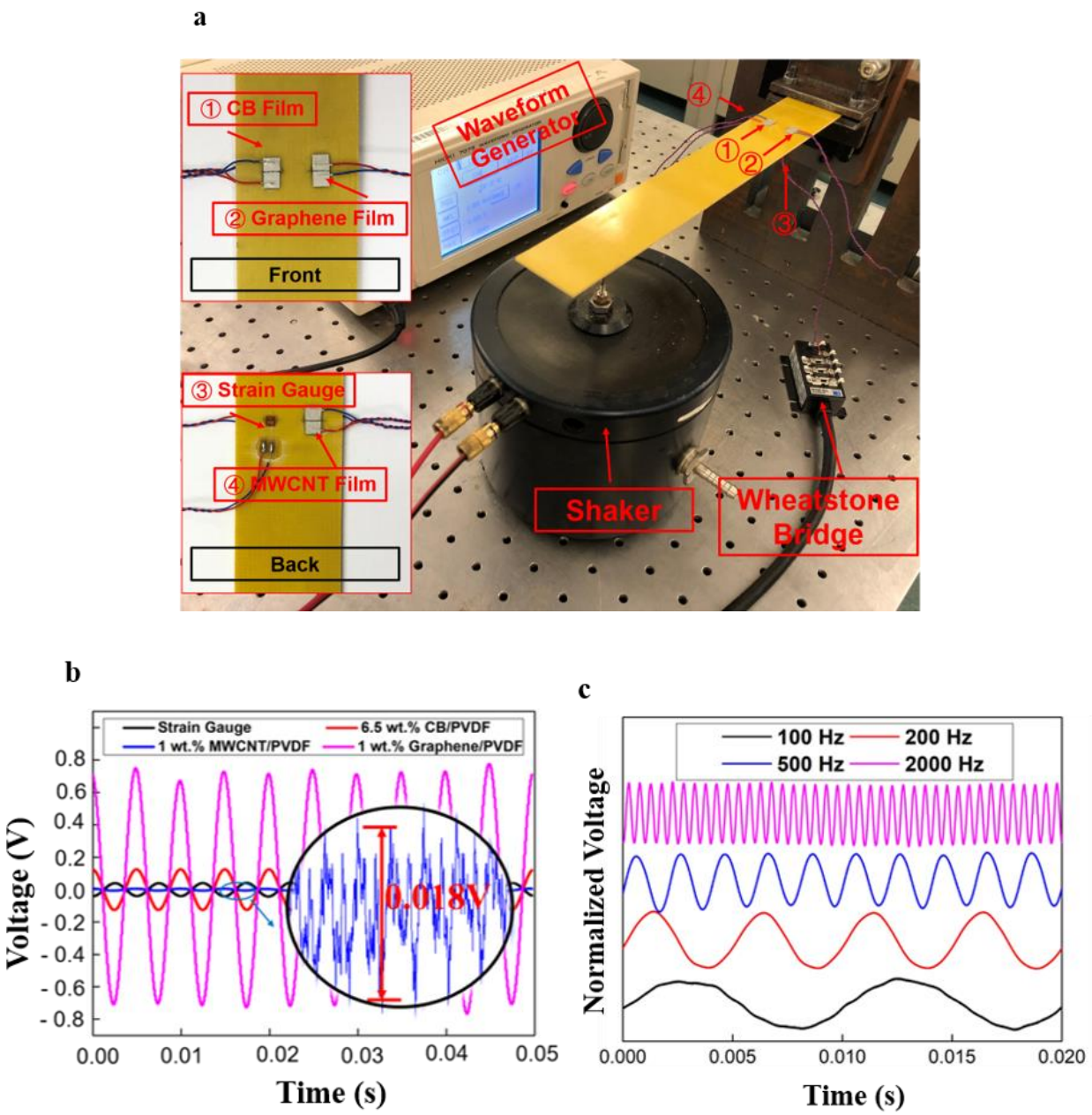

Fig. 5. (a) Schematic of experimental setup; (b) electromechanical responses of nanocomposite samples of three nanofiller genres to a vibration at 200 Hz; (c) response of graphene/PVDF-based nanocomposite sample at representative frequencies from 100 Hz to 2 kHz (signals normalized by respective maximum magnitudes)

2.5. *Mechanism of sensing ultrasound*

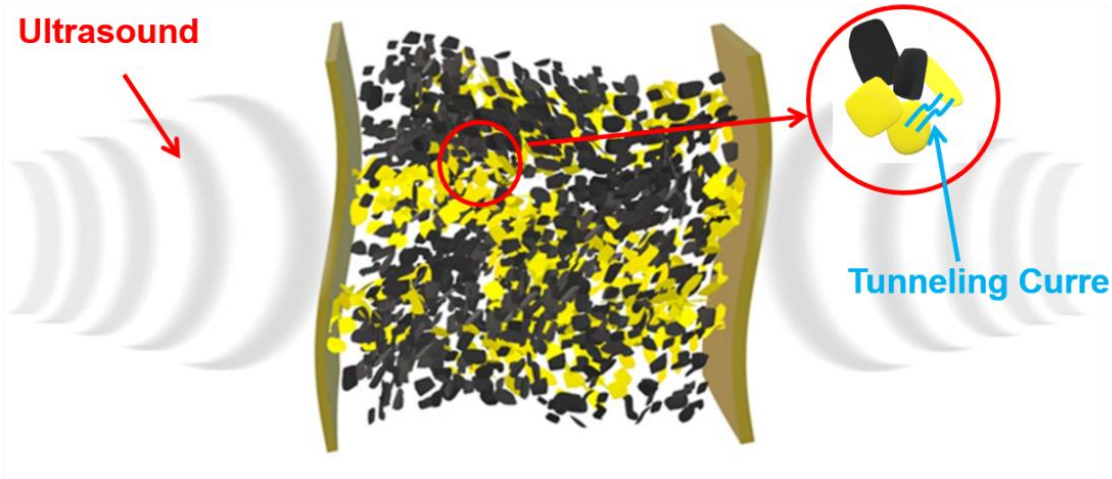

Fig. 6. Schematic illustration of ultrasound propagation triggering tunneling current in graphene nanoparticle-formed conductive network at its percolation threshold (from molecular dynamics-based simulation).

Up to this point, the graphene nanoparticle/PVDF nanocomposites at their percolation threshold had been demonstrated responsive to a dynamic disturbance up to 2000 Hz, with measurement reversibility and repeatability yet without hysteresis and deviation. Importantly, the reversibility underpinned the speculation that under a dynamic disturbance (e.g., the strain induced by ultrasound), the pivotal sensing mechanism of the nanocomposite piezoresistive sensors is the tunneling effect triggered in the conductive network formed by nanofillers (as well as their aggregations) [24-26]. At nanoscale, the tunneling effect occurs when neighboring nanoparticles are in close proximity (usually of the order of several nanometers) but not in a direct contact. As shown in **Fig. 6**, this can be illustrated by a molecular dynamics-based simulation: when an ultrasound signal traverses the nanocomposites, the dynamic disturbance triggers the tunneling of charged carriers, locally altering the conductivity of the percolating network. Although the energy carried is of an ultralow amplitude, an ultrasound signal suffices to promote measurable modulation of the graphene nanoparticle-formed conductive network at its percolation threshold, engendering a

tunneling current to subsequently alter the electrical resistance manifested. For the relevant work, refer to the authors' earlier publication [32].

It is relevant to point out that the PVDF – the matrix of the nanocomposites – has been traditionally used to develop strain sensors [15], by virtue of its superior flexibility and greater ease of handling than many other candidate materials such as PZT. In this study, however, PVDF was used solely as a matrix to accommodate dispersed graphene nanoparticles. Here, to exclude the possibility that the piezoresistivity manifested by the nanocomposites in response to ultrasound could originate from the PVDF matrix, an X-ray diffraction (XRD) test was conducted. XRD analysis was implemented at room temperature on an XRD platform (X'Pert Pro, PANalytical) with a specular reflection mode (Cu Ka radiation) and a scanning angle varying from 15° to 29° (at the scanning rate of 4° s^{-1}).

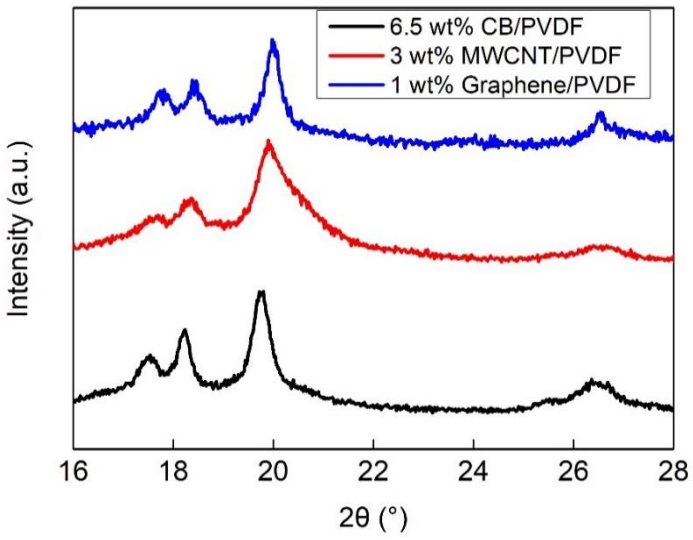

Fig. 7. XRD pattern of the three nanocomposite genres (2θ: scanning angle).

Fig. 7 presents XRD results for the nanocomposites with the three representative nanofiller types, demonstrating that the fabricated nanocomposites, regardless of nanofiller type, feature a pattern of α-crystal with a nonpolar crystal structure. This finding implies that the PVDF in the nanocomposites, as a matrix, does not cause remarkable piezoelectricity – because only a polar crystal (such as β-crystals) can lead to piezoelectricity [15, 37-39]. The nonpolar crystal structure

can be attributed partly to the solution-mixing process adopted in this study for compounding graphene nanoparticles into PVDF. Thus, once any change in conductivity is perceived, it can be fully attributed to the change in the percolating network induced by ultrasound as a result of the tunneling effect, rather than due to a response from PVDF itself.

2.6. *Integration of functional sensors*

The aqueous graphene nanoparticle/PVDF nanocomposites were directly sprayed on a substrate film using a screen-printing approach. In that approach, a polymer film with desired cutouts was pre-fabricated (serving as a molding layer) and pressed onto the substrate film. The thickness of the polymer film and cutouts was deliberately designed, determining the thickness and size of the sensors finally deposited on the substrate. After sufficient curing, the molding layer was peeled off, leaving individual nanocomposite flakes on the substrate, each of which measured 10 mm × 5 mm × ~5 μm after degassing and curing. These flakes exhibit excellent resilience and flexibility (**Fig. 8**), highlighting their potential for use on non-flat structural surfaces and human bodies as wearable devices. Two fine finger electrodes for each sensor were also screen-printed on the substrate film using a silk printing method. With an electrode pair, each printed nanocomposite flake was functionalized as a self-contained sensor. In the thin film modality, such produced sensors were resilient, able to adapt to a curved structural surface for *in-situ* acquisition of ultrasound – a challenging task for conventional PZT ultrasound sensors due to their high stiffness. These merits of the produced sensor were not constrained by the material properties (metals or composites) or geometry (flat or curved) of the recipient structure to be sprayed on.

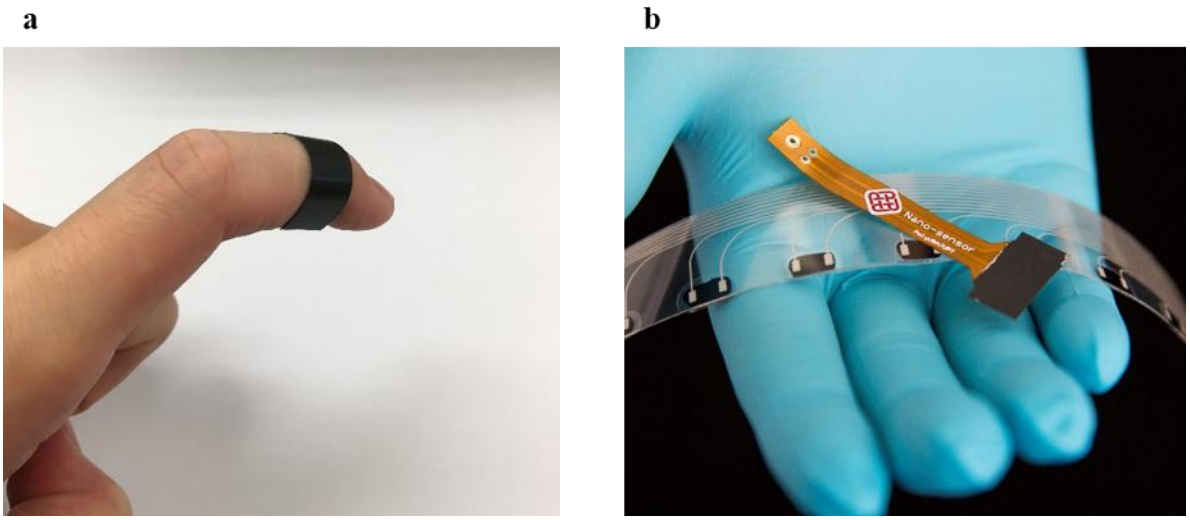

Fig. 8. Produced spray-on nanocomposite sensor. a) a screen-printed nanocomposite flake, showing good resilience, and b) a self-contained sensor with electrode pair.

2.7. *In-situ acquisition of ultrasound*

The self-contained, dedicated signal acquisition system was developed on a PXI (PCI eXtensions for Instrumentation) bus platform (NI® PXIe-1071). The system featured mainly a signal amplification module, an electronic amplifier circuit, a series of filters and a signal conversion circuit for converting measured piezoresistivity to electrical signals, a waveform generator (NI® PXIE-1071) (for exciting ultrasound via PZT wafer), a linear power amplifier (Ciprian® US-TXP-3), and an oscilloscope (Agilent® DSO9064A).

Intrinsically, an ultrasound signal is low in magnitude and prone to contamination from ambient noise and measurement uncertainties. With this consideration a dedicated signal conditioner device was developed, to be used in conjunction with the fabricated sensors. The device consisted mainly of a high-pass filter and an electrical Wheatstone bridge. In a frequency sweep test, a group of ultrasound signals, 5-cycle *Hanning*-function-modulated sinusoidal tonebursts, with frequency varying from 2 kHz to 1.4 MHz with an increment of 1 kHz, were emitted into a glass-fiber-epoxy laminate panel (600 mm × 600 mm × 2 mm) via a surface-mounted PZT wafer (PSN-33, Ø8 mm, 0.48 mm thick). Eight nanocomposite sensors were adhered to the panel at eight

arbitrarily selected positions. For verification and calibration, another eight PZT wafers were respectively collocated adjacent to each nanocomposite sensor, to capture ultrasound signals simultaneously. A schematic of the experimental setup is shown in **Fig. 9**a. By way of illustration, the signals respectively captured by one of the eight nanocomposite sensors and its adjacent PZT wafer are compared at 200 kHz (**Fig. 9**b) and 1.2 MHz (**Fig. 9**c). These signals were processed with a first-order Butterworth filter to remove measurement noise. In the processed signals, quantitative coincidence between PZT- and nanocomposite sensor-captured signals can be observed, in particular, for the first-arriving wave component – that is, the zeroth-order symmetric Lamb wave mode guided by the panel (denoted by S_0 hereinafter). Discrepancies in signals captured by the two types of sensor, particularly under the excitation of 1.2 MHz, can be attributed to the distinct sensing mechanisms: a PZT wafer measures changes in piezoelectric properties, whereas the nanocomposite sensor registers variation in piezoresistive properties based on the tunneling effect.

Further, the spectra of signals perceived by the nanocomposite sensor are presented over a frequency-time domain via short-time Fourier transform, separately deployed in a lower frequency range (50 kHz~450 kHz, **Fig. 9**d) and a higher frequency range (500 kHz~1.4 MHz, **Fig. 9**e), both showing high consistency of the sensor at any monochromatic frequency in a broadband up to 1.4 MHz. These observations authenticate the excellent performance of the fabricated sensor in responding to ultrasound across a wide spectrum. Not only the S_0 mode but also other wave modes (e.g., antisymmetric Lamb wave mode, A_0) can be captured by the nanocomposite sensor.

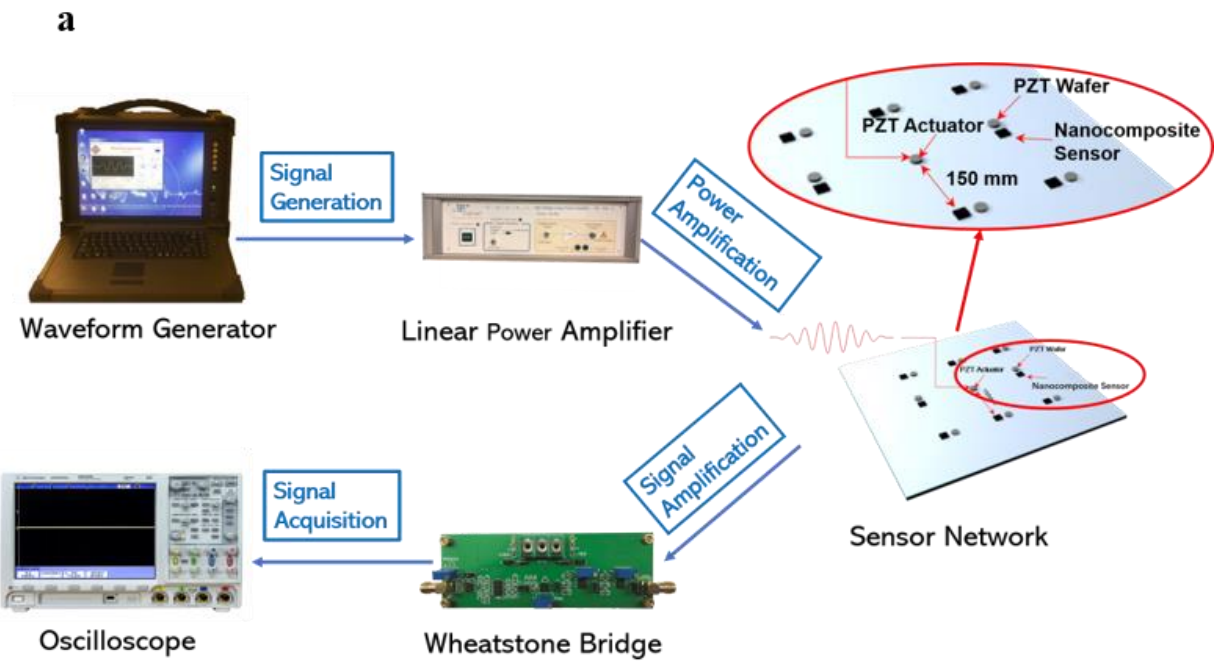
a
Waveform Generator
Signal Generation
Linear Power Amplifier
Power Amplification
PZT Wafer
PZT Actuator
Nanocomposite Sensor
150 mm
Sensor Network
Signal Amplification
Signal Acquisition
Wheatstone Bridge
Oscilloscope

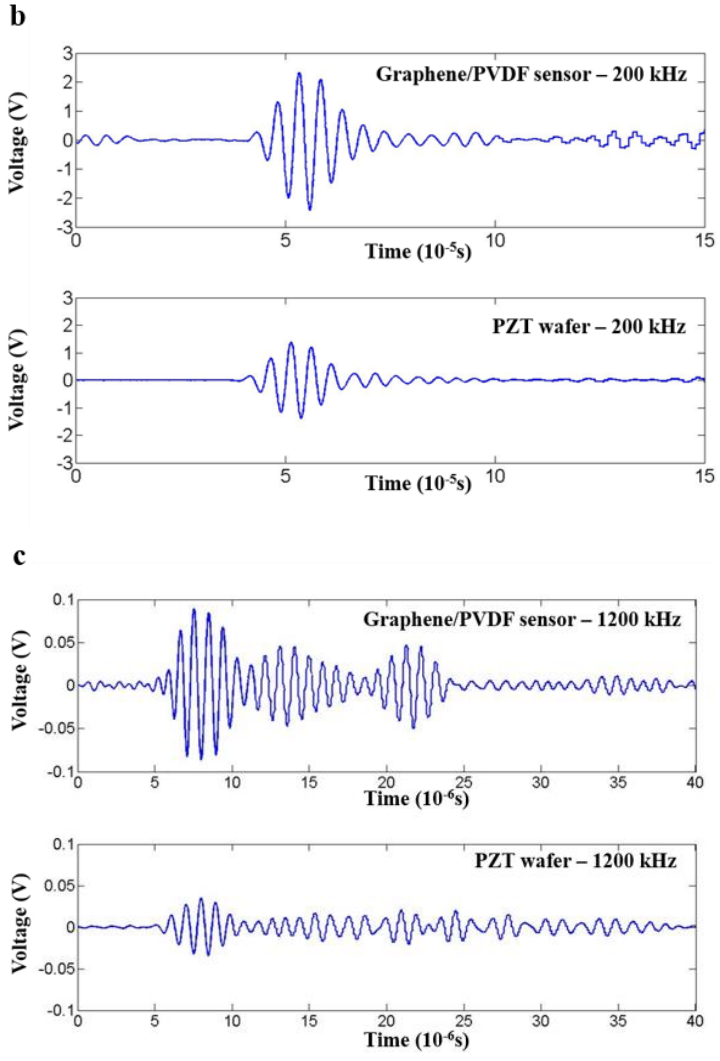
b
Graphene/PVDF sensor – 200 kHz
PZT wafer – 200 kHz
Voltage (V)
Time (10-5s)
c
Graphene/PVDF sensor – 1200 kHz
PZT wafer – 1200 kHz
Time (10-6s)

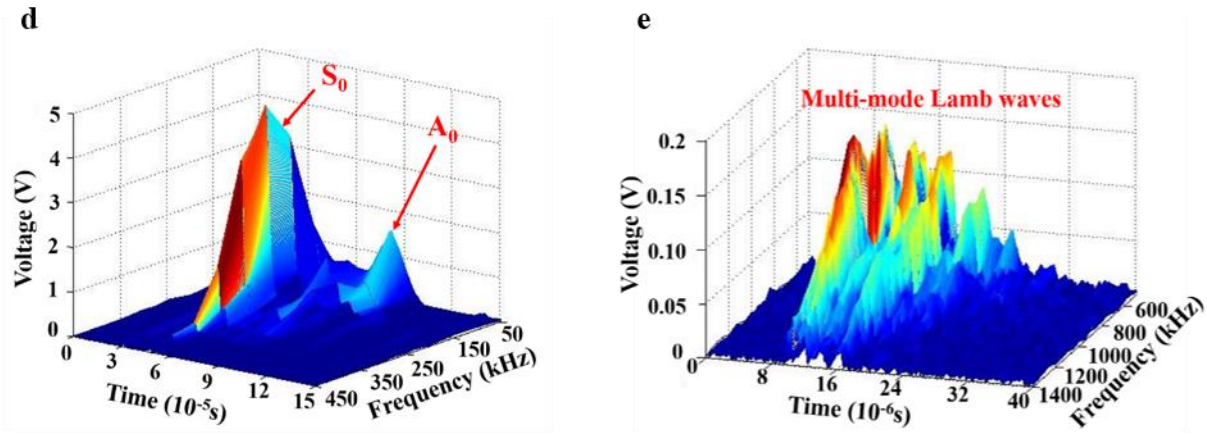

Fig. 9. Performance of the nanocomposite sensor for acquisition of broadband ultrasound against conventional PZT wafer: a) schematic of experimental setup; signals captured by a nanocomposite sensor and PZT wafer at b) 200 kHz and c) 1.2 MHz; spectra (obtained using short-time Fourier transform) of broadband signals captured by the nanocomposite sensor in a frequency range of d) 50 kHz~450 kHz and e) 500 kHz~1.4 MHz.

3. Conclusions

Through a frequency range up to 1.4 MHz, the graphene/PVDF nanocomposite sensor outperforms its counterparts made of MWCNTs or CB, exhibiting the highest sensitivity and greatest gauge factor (~55.0 ± 0.6 at percolation threshold, **Fig. 4a**) to a broadband ultrasound, compared with the lowest gauge factor of the MWCNT-based nanocomposite sensor. The gauge factor of the sensor is also much greater than that of a conventional metal-foil strain gauge that is usually ~2. A higher gauge factor guarantees superior sensitivity of the sensor to an ultrasound with an ultralow magnitude (of a microstrain order). Compared with 0-D CB or 1-D MWCNT, the 2-D structure of the graphene nanoparticle is conducive to decreasing the possibility of nanofiller entanglement and aggregation and is beneficial to the formation of an even, stable, and uniform percolating network within the nanocomposites, in which the tunneling effect plays a dominant role in making the sensor responsive to disturbance in an ultrasonic regime. Moreover, the highest SSA of graphene nanoparticles augments the number of contact points in the matrix. The matrix, PVDF,

possesses a higher elastic modulus than that of traditional rubber-based materials and is therefore capable of responding more rapidly to a dynamic load with higher frequency. The somewhat frequency-independent viscoelastic traits of the matrix allow it to respond inherently easily to a dynamic disturbance without prominent hysteresis. Together, these features make the graphene nanoparticle/PVDF nanocomposite sensor most sensitive to broadband ultrasound.

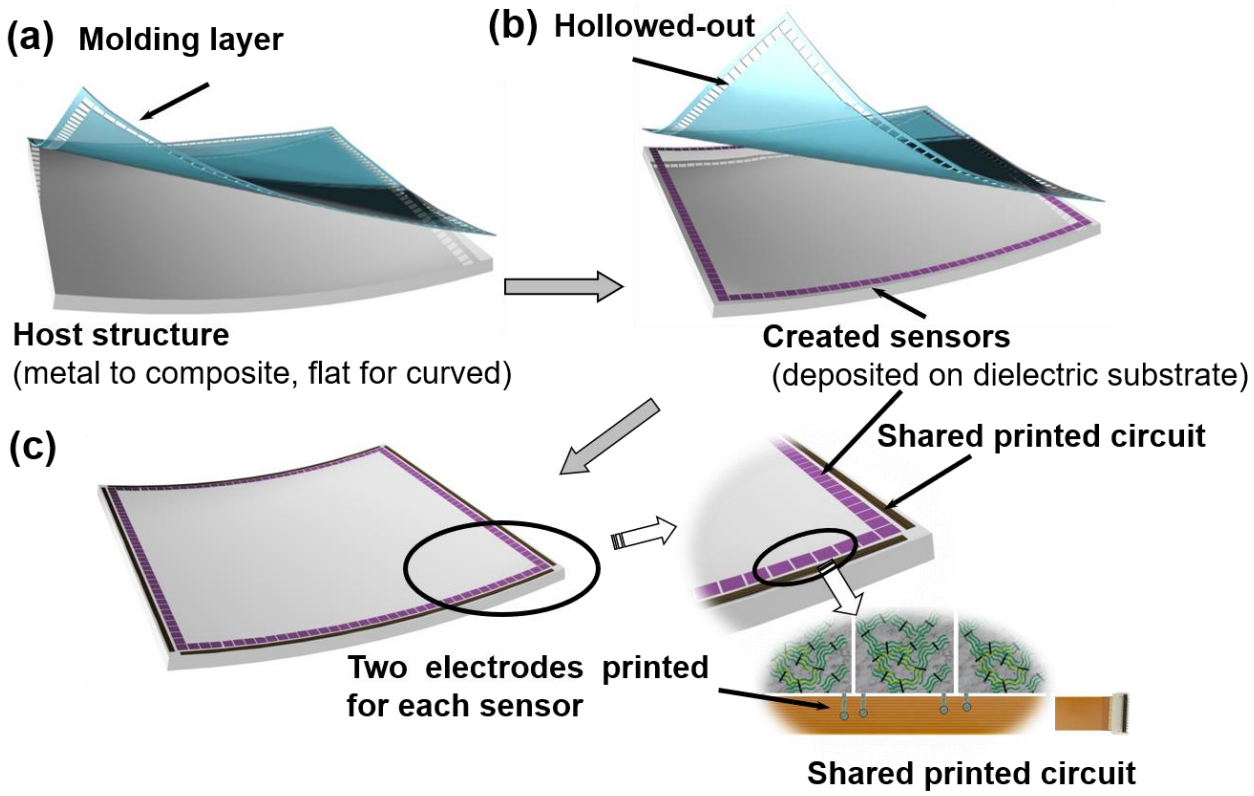

Fig. 10. Schematic of the spray-on process for developing a dense sensor network using the graphene nanoparticle/PVDF nanocomposites: a) molding layer on the host structure, b) the hollowed-out pattern of the molding layer is deliberately designed to determine the final sprayed sensor network, including size, thickness, location, and shape of each sensing element, and the total number of sensing elements in the network, and c) after the graphene nanoparticle/PVDF nanocomposites are sprayed on the host structure, the molding layer is peeled off, leaving the spray-on sensor network on the host structure.

An additional merit of the nanocomposite sensor compared with conventional PZT wafers is its independence of the frequency of an ultrasound signal to respond to. In a PZT wafer, its resonant frequency (e.g., the resonant frequency in the PZT used in this study was 300 kHz) significantly affects the captured signals, and the signals can be anamorphic provided the resonant frequency of the sensor is distant from the central frequency of the signal. That trait in conventional PZT sensors greatly narrows the operational frequency band. Also, the fabricated nanocomposites can be coated or sprayed onto a structure directly and deployed in large quantities to form a dense, spray-on *in-situ* sensing network in a cost-effective manner, as schematically depicted in **Fig. 10**, in which the circuits (including the finger electrode pair for each sensor used to interlink the sensors in the sensor network) can also be deposited on the structural surface using an inkjet printing approach.

With its extra-lightweight, the sensor network thus produced imposes negligible volume and weight penalty on the host structure, yet can acquire rich information, circumventing the deficiency of conventional sensor networks with sparsely distributed sensors (*e.g.*, PZT) in achieving a compromise between 'sensing effectiveness' and 'sensing cost'. By 'communicating' with each other cooperatively, the networked sensors holistically and collectively perceive ambient information and system parameters, with extra redundancy of data acquisition. Sensor networks can be tailored to accommodate diverse needs such as ultrasonics-based health monitoring (for both human and engineering assets), tactile sensing, and wearable apparatus.

Acknowledgements

This project is supported by the Hong Kong Research Grants Council via a General Research Fund (No. 15214414, 15201416 and 15212417). The work done at City University of Hong Kong is supported by the Hong Kong Research Grants Council under CityU 11216515 and CityU

11207416. Menglong LIU thanks the Institute of High Performance Computing for the use of computational resources in this research.

References

[1] D. Kang, P.V. Pikhitsa, Y.W. Choi, C. Lee, S.S. Shin, L. Piao, et al., Ultrasensitive mechanical crack-based sensor inspired by the spider sensory system, Nature 516(7530) (2014) 222-6.

[2] X. Chong, L. Jia, F. Tian-Ming, D. Xiaochuan, Z. Wei, M.L. Charles, Three-dimensional macroporous nanoelectronic networks as minimally invasive brain probes, Nat Mater 14(12) (2015) 1286-1292.

[3] S. Gregor, C.K.T. Benjamin, M. Jianguo, L.A. Anthony, K. Do Hwan, W. Huiliang, et al., Flexible polymer transistors with high pressure sensitivity for application in electronic skin and health monitoring, Nat Commun 4 (2013) 1859.

[4] S. Imani, A.J. Bandodkar, A.M.V. Mohan, R. Kumar, S. Yu, J. Wang, et al., A wearable chemical-electrophysiological hybrid biosensing system for real-time health and fitness monitoring, (2016) 11650.

[5] D.-H. Kim, N. Lu, R. Ma, Y.-S. Kim, R.-H. Kim, S. Wang, et al., Epidermal electronics. (RESEARCH ARTICLES)(Author abstract)(Report), Science 333(6044) (2011) 838.

[6] J. Kim, M. Lee, H. Shim, R. Ghaffari, H. Cho, D. Son, et al., Stretchable silicon nanoribbon electronics for skin prosthesis, Nat Commun 5 (2014) 5747.

[7] P. Lijia, C. Alex, Y. Guihua, W. Yaqun, I. Scott, A. Ranulfo, et al., An ultra-sensitive resistive pressure sensor based on hollow-sphere microstructure induced elasticity in conducting polymer film, Nat Commun 5 (2014) 3002.

[8] C. Shumao, P. Haihui, A.W. Spencer, W. Zhenhai, M. Shun, C. Jingbo, et al., Ultrahigh sensitivity and layer-dependent sensing performance of phosphorene-based gas sensors, Nat Commun 6(1) (2015) 8632.

[9] Y. Takeo, H. Yuhei, Y. Yuki, Y. Yoshiki, I.-N. Ali, N.F. Don, et al., A stretchable carbon nanotube strain sensor for human-motion detection, Nat Nanotechnol 6(5) (2011) 296.

[10] T. Yang, W. Wang, H. Zhang, X. Li, J.D. Shi, Y. He, et al., Tactile Sensing System Based on Arrays of Graphene Woven Microfabrics: Electromechanical Behavior and Electronic Skin Application, Acs Nano 9(11) (2015) 10867-10875.

[11] C.S. Boland, U. Khan, C. Backes, A. Neill, J. McCauley, S. Duane, et al., Coleman, Sensitive, high-strain, high-rate bodily motion sensors based on graphene-rubber composites, Acs Nano 8(9) (2014) 8819.

[12] Y. Cheng, R. Wang, J. Sun, L. Gao, A Stretchable and Highly Sensitive Graphene‐Based Fiber for Sensing Tensile Strain, Bending, and Torsion, Adv Mater 27(45) (2015) 7365-7371.

[13] X. Gui, A. Cao, J. Wei, H. Li, Y. Jia, Z. Li, et al., Soft, highly conductive nanotube sponges and composites with controlled compressibility, Acs Nano 4(4) (2010) 2320.

[14] D. Lipomi, M. Vosgueritchian, B. Tee, S. Hellstrom, J. Lee, C. Fox, Z. Bao, Skin-like pressure and strain sensors based on transparent elastic films of carbon nanotubes, Nat Nanotechnol 6(12) (2011) 788-92.

[15] Z. Lou, S. Chen, L. Wang, K. Jiang, G. Shen, An ultra-sensitive and rapid response speed graphene pressure sensors for electronic skin and health monitoring, Nano Energy 23 (2016) 7-14.

[16] Y. Qin, Q. Peng, Y. Ding, Z. Lin, C. Wang, Y. Li, et al., Lightweight, Superelastic, and Mechanically Flexible Graphene/Polyimide Nanocomposite Foam for Strain Sensor Application, Acs Nano 9(9) (2015) 8933.

[17] J. Sebastian, N. Schehl, M. Bouchard, M. Boehle, L. Li, A. Lagounov, et al., Health monitoring of structural composites with embedded carbon nanotube coated glass fiber sensors, Carbon 66(C) (2013) 191.

[18] G. Shu, S. Willem, W. Yongwei, C. Yi, T. Yue, S. Jye, et al., A wearable and highly sensitive pressure sensor with ultrathin gold nanowires, Nat Commun 5 (2014) 3132.

[19] E.T. Thostenson, T.W. Chou, Carbon Nanotube Networks: Sensing of Distributed Strain and Damage for Life Prediction and Self Healing, Adv Mater 18(21) (2006) 2837-2841.

[20] H. Yazdani, K. Hatami, E. Khosravi, K. Harper, B.P. Grady, Strain-sensitive conductivity of carbon black-filled PVC composites subjected to cyclic loading, Carbon 79(C) (2014) 393-405.

[21] L. Qiu, M. Bulut Coskun, Y. Tang, J.Z. Liu, T. Alan, J. Ding, et al., Ultrafast Dynamic Piezoresistive Response of Graphene‐Based Cellular Elastomers, Adv Mater 28(1) (2016) 194-200.

[22] S. Liu, X. Wu, D.D. Zhang, C.W. Guo, P. Wang, W. Hu, X. Li, et al., Ultrafast Dynamic Pressure Sensors Based on Graphene Hybrid Structure, ACS Appl. Mater. Interfaces 9(28) (2017) 24148-24154.

[23] M. Amjadi, K.U. Kyung, I. Park, M. Sitti, Stretchable, Skin‐Mountable, and Wearable Strain Sensors and Their Potential Applications: A Review, Adv Funct Mater 26(11) (2016) 1678-1698.

[24] N. Hu, T. Itoi, T. Akagi, T. Kojima, J. Xue, C. Yan, et al., Ultrasensitive strain sensors made from metal-coated carbon nanofiller/epoxy composites, Carbon 51(C) (2013) 202-212.

[25] N. Hu, Y. Karube, C. Yan, Z. Masuda, H. Fukunaga, Tunneling effect in a polymer/carbon nanotube nanocomposite strain sensor, Acta Mater 56(13) (2008) 2929-2936.

[26] N. Hu, Y. Karube, M. Arai, T. Watanabe, C. Yan, Y. Li, et al., Investigation on sensitivity of a polymer/carbon nanotube composite strain sensor, Carbon 48(3) (2010) 680-687.

[27] J. Zhao, G. Wang, R. Yang, X. Lu, M. Cheng, C. He, et al., Tunable piezoresistivity of nanographene films for strain sensing, Acs Nano 9(2) (2015) 1622-1629.

[28] M. Amjadi, M. Turan, C.P. Clementson, M. Sitti, Parallel Microcracks-based Ultrasensitive and Highly Stretchable Strain Sensors, ACS Appl. Mater. Interfaces 8(8) (2016) 5618-5626.

[29] S. Gong, D. Lai, Y. Wang, L. Yap, K. Si, Q. Shi, et al., Tattoo like Polyaniline Microparticle-Doped Gold Nanowire Patches as Highly Durable Wearable Sensors, ACS Appl. Mater. Interfaces 7(35) (2015) 19700-19708.

[30] A.I. Oliva-Avilés, F. Avilés, V. Sosa, Electrical and piezoresistive properties of multi-walled carbon nanotube/polymer composite films aligned by an electric field, Carbon 49(9) (2011) 2989-2997.

[31] X. Xiao, L. Yuan, J. Zhong, T. Ding, Y. Liu, Z. Cai, et al., High‐Strain Sensors Based on ZnO Nanowire/Polystyrene Hybridized Flexible Films, Adv Mater 23(45) (2011) 5440-5444.

[32] Z. Zeng, M. Liu, H. Xu, Y. Liao, F. Duan, L.-m. Zhou, et al., Ultra-broadband frequency responsive sensor based on lightweight and flexible carbon nanostructured polymeric nanocomposites, Carbon 121 (2017) 490-501.

[33] F. Bonaccorso, L. Colombo, G. Yu, M. Stoller, V. Tozzini, A. Ferrari, et al., Graphene, related two-dimensional crystals, and hybrid systems for energy conversion and storage, Science 347 (2015) 6217.

[34] J. Chen, J. Foiret, J. G. Minonzio, M. Talmant, Z. Su, L. Cheng, et al., Measurement of guided mode wavenumbers in soft tissue−bone mimicking phantoms using ultrasonic axial transmission, Physics in Medicine and Biology 57 (2012) 3025-3037.

[35] J. Chen, and Z. Su, On ultrasound waves guided by bones with coupled soft tissues: a mechanism study and in vitro calibration, Ultrasonics 54 (2014) 1186-1196.

[36] H. Xu, Z Zeng, Z. Wu, K. Zhou, Z. Su, Y. Liao, et al., Broadband dynamic responses of flexible carbon black/poly(vinylidene fluoride) nanocomposites: A sensitivity study, Compos Sci Technol 149 (2017) 246-253

[37] C. Chang, V.H. Tran, J. Wang, Y.-K. Fuh, L. Lin, Direct-write piezoelectric polymeric nanogenerator with high energy conversion efficiency, Nano Lett 10(2) (2010) 726.

[38] L. Chenhong, F. Jian, S. Hao, D. Xin, L. Tong, High-sensitivity acoustic sensors from nanofibre webs, Nat Commun 7 (2016) 11108.

[39] P. Xiao, N. Yi, T. Zhang, Y. Huang, H. Chang, Y. Yang, et al., Construction of a Fish‐like Robot Based on High Performance Graphene/PVDF Bimorph Actuation Materials, Adv Sci 3(6) (2016) 1500438.